Multichannel Optical Signal Processing in NRZ Systems Based on a Frequency-Doubling Optoelectronic Oscillator

Shilong Pan, *Member, IEEE*, and Jianping Yao, *Senior Member, IEEE*

***Abstract*—Optical signal processing, including clock recovery, nonreturn-to-zero (NRZ) to return-to-zero (RZ) or to carrier-suppressed return-to-zero (CSRZ) format conversions, serial-to-parallel conversion, and optical regeneration in NRZ systems using a frequency-doubling optoelectronic oscillator (OEO) is investigated. The key device in the OEO is a dual-output intensity modulator (IM), which is implemented using a polarization modulator (PolM). If a continuous-wave (CW) probe along with a multichannel NRZ signal is injected into the OEO, an electrical clock at half the data rate of the NRZ signal will be generated. When the electrical clock is fed back into the PolM-based IM, it will modulate the later injected CW probe and the NRZ signal, thus carving the NRZ signal to be an RZ/CSRZ signal at the same data rate or an RZ signal at half the data rate of the NRZ signal. Meanwhile, the CW probe is also carved to be an optical pulse train with a frequency equal to the data rate or half the data rate of the NRZ signal. Multichannel line-rate and prescaled clock recovery, NRZ-to-RZ/CSRZ conversion, 1:2 serial-to-parallel conversion, and synchronous-modulation-based regeneration are thus realized. An experiment is performed with all the aforementioned signal processing functions verified.**

***Index Terms*—Carrier-suppressed return-to-zero (CSRZ), clock recovery, dense wavelength-division multiplexing (DWDM), format conversion, nonreturn-to-zero (NRZ), optical communications, optoelectronic oscillator (OEO), polarization modulator (PolM), regeneration, return-to-zero (RZ), serial-to-parallel conversion.**

I. Introduction

FUTURE high-speed and large-capacity optical networks are likely to adopt the advantages offered by both wavelength-division multiplexing (WDM) and optical time-division multiplexing (OTDM) technologies. Several modulation formats, such as nonreturn-to-zero (NRZ), return-to zero (RZ), and carrier-suppressed return-to-zero (CSRZ) [1], may be selectively used to accommodate the different requirements of the networks. Optical format conversion is thus highly desirable to ensure a transparent connection of optical networks operating with different modulation formats [2]–[6]. On the other hand, when a high-speed optical signal is transmitted in an optical fiber, it undergoes various distortions due to the impairments caused by system noise, attenuation, fiber dispersion, and nonlinearity. To overcome these impairments, optical signal regeneration is proposed to restore the signal quality [7]–[9]. Since the bit rate of an optical signal, in future network, may be too high to be processed by a signal processing module, e.g., a buffering or label-recognizing module, optical serial-to-parallel conversion (also known as demultiplexing in an OTDM system) is needed to convert a fast incoming serial signal to multiple slow parallel signals [10], [11]. Optoelectronic oscillators (OEOs) are good candidates to realize the aforementioned signal processing functions [12]–[26]. For instance, to perform optical NRZ-to-RZ format conversion using conventional techniques [3]–[5], two-stage processing is always needed. In such techniques, clock extractions are implemented in the first stage by converting an NRZ signal to a pseudo-RZ (PRZ) signal followed by an RZ clock extraction scheme. Then, wavelength conversion is applied to duplicate the information of the NRZ signal to the optical clock train at a new wavelength. If an OEO is applied, the procedure can be greatly simplified, since the OEO can simultaneously realize NRZ clock extraction and NRZ-to-RZ format conversion [12].

An OEO is an optoelectronic feedback loop consisting of an intensity modulator (IM), an optical fiber delay line [or an electrical phase shifter (PS)], a photodetector (PD), an electrical amplifier (EA), and a high-Q electrical bandpass filter (EBPF) [13]. If the loop gain is higher than the loss, when a continuous-wave (CW) light is injected into the IM, the OEO will start to oscillate at one of its eigenmodes determined by the center frequency of the EBPF. The spacing between two adjacent eigenmodes is determined by the total length of the loop. If an incoming data signal containing a clock with a frequency near the oscillating frequency and a sufficiently large power is introduced into the OEO loop, the OEO will be injection locked. The clock signal is then extracted, while other frequency components in the data signal are suppressed [15]–[17]. With the extracted high-quality line-rate or prescaled clock, several optical signal processing functions, such as NRZ-to-RZ format conversion [12], OTDM demultiplexing [18], [19], and synchronous-modulation-based regeneration [20], can be directly performed in the OEO.

The major limitation of a conventional OEO for optical signal processing in a high-speed optical communication system is that it can only operate at a maximum frequency which is limited by the bandwidth of the devices in the OEO loop. For instance, to extract the line-rate clock from a 40-Gb/s signal or to perform 40-Gb/s NRZ-to-RZ format conversion, the devices

Manuscript received September 1, 2009; revised October 21, 2009 and November 7, 2009; accepted November 12, 2009. Date of publication March 22, 2010; date of current version October 6, 2010. This work was supported by the Natural Sciences and Engineering Research Council of Canada.

The authors are with the Microwave Photonics Research Laboratory, School of Information Technology and Engineering, University of Ottawa, Ottawa, ON K1N 6N5, Canada (e-mail: span@site.uottawa.ca; jpyao@site.uOttawa.ca).

Color versions of one or more of the figures in this paper are available online at http://ieeexplore.ieee.org.

Digital Object Identifier 10.1109/JSTQE.2009.2037159

in the OEO loop, i.e., the IM, the PD, the EAs, the electrical PS, and the connectors, should have a bandwidth up to 40 GHz. To extend the operation frequency using lower frequency devices, frequency-doubling OEOs have recently been proposed [21]–[26]. In 2005, Sakamoto *et al.* successfully demonstrated a frequency-doubling OEO by biasing a $LiNbO_3$ Mach–Zehnder modulator (MZM) at the minimum transmission point (MITP) [21], which was further applied for optical prescaled clock recovery in an RZ system [22]. To obtain the feedback signal required for optoelectronic oscillation in their approach, the frequency-doubled component in the optical signal was detected by a wideband PD, amplified by a high-frequency EA, and then divided into the oscillating frequency by an electrical frequency divider. Due to the demands for high-frequency electrical devices, the approach in [21] and [22] did not really increase the operation frequency. By using the wavelength-dependent nature of the half-wave voltage of a $LiNbO_3$ MZM, Shin *et al.* proposed another frequency-doubling OEO [23]. In their system, two CW lasers operating at 1550 and 1310 nm were used. The bias voltage was carefully adjusted such that the modulation was performed at the quadrature transmission point (QTP) for the wavelength at 1310 nm to produce a low-frequency feedback signal, and the modulation was performed at the MITP for the wavelength at 1550 nm to generate a frequency-doubled signal. The key limitation associated with the operation of an MZM at the MITP is the bias-drifting problem, which makes the system unstable, or a sophisticated control circuit is needed to stabilize the operation. In addition, two optical sources at two different wavelengths are needed, thus making the system more complicated and costly. To overcome the problems, we have recently proposed a frequency-doubling OEO using a polarization modulator (PolM) without the need for high-frequency electrical devices and an additional optical light source [24]. The frequency-doubling OEO was successfully applied to recover both the line-rate and prescaled clock from a degraded RZ signal [25]. The use of the frequency-doubling OEO to perform serial-to-parallel conversion in an RZ system was also recently demonstrated [26].

In this paper, a PolM-based frequency-doubling OEO is applied to perform multichannel optical signal processing in an NRZ system. Several optical signal processing functions, such as prescaled and line-rate clock recovery, NRZ-to-RZ/CSRZ conversion, 1:2 serial-to-parallel conversion, and synchronous-modulation-based optical regeneration, are implemented in an NRZ system using only low-frequency devices. The paper is organized as follows. In Section II, we first describe the PolM-based frequency-doubling OEO and study the basic operation principle for optical clock recovery, NRZ-to-RZ/CSRZ conversion, 1:2 serial-to-parallel conversion, and optical signal regeneration in a multichannel NRZ system. In Section III, the experimental setup is introduced. In Section IV, a prescaled clock at 6.2 GHz and a line-rate clock at 12.4 GHz are experimentally extracted from a degraded 12.4-Gb/s NRZ signal. Then, NRZ-to-RZ/CSRZ conversion and 1:2 serial-to-parallel conversion are demonstrated. The regeneration property of the scheme is investigated by comparing the bit error rates (BERs) of the degraded signal and the later regenerated signal. To demonstrate that the OEO is suitable for multichannel optical signal processing, an experiment in which the OEO is in dual-wavelength operation with wavelength spacing varying from 0.4 to 18 nm is studied. A conclusion is drawn in Section IV.

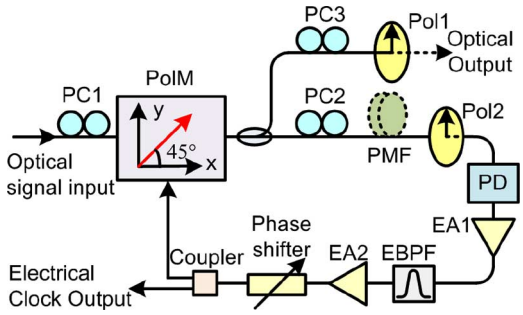

Fig. 1. Schematic diagram of the PolM-based frequency-doubling OEO.

II. Operation Principle

The schematic diagram of the frequency-doubling OEO is shown in Fig. 1. An input optical signal is fiber coupled to a PolM via a polarization controller (PC) (PC1). The PolM is connected to two polarizers via two other PCs (PC2 and PC3). The PolM in conjunction with the PCs and the polarizers is equivalent to a two-output-port IM [25]. One output of the IM is fed back to the PolM via the RF port to form an OEO loop. A PD is used in the OEO loop to perform optical-to-electrical conversion. To select the oscillation frequency, a narrowband EBPF is incorporated. Two EAs are inserted before and after the EBPF to ensure that the loop gain is higher than unity, which is the condition required to guarantee oscillation.

A. Single-Channel Signal Injection

Based on [25], to perform prescaled or line-rate clock recovery using the frequency-doubling OEO, the input optical signal must have a distinct clock component with a frequency near f_0 or $2f_0$ (assume f_0 is the oscillating frequency of the free-running OEO). It is well known that the electrical spectrum of an ideal NRZ data contains no clock components. In the real case, however, a weak clock component is always produced when the NRZ signal is converted from the electrical domain to the optical domain at an electrooptic MZM, since the transmission function of an MZM is not ideally linear. The nonlinear process in the MZM would mix the spectral components in the optical signal, e.g., f_1 and $f_1 + f_m$ (f_m is the bit rate, which is close to $2f_0$), to generate a clock component at f_m. In addition, the imperfect multiplexing in the electrical domain to generate the high-bit-rate electrical NRZ signal would also create the clock component [27]. Fig. 2 shows the eye diagrams and electrical spectra of a typical 12.4-Gb/s optical NRZ signal before and after transmission. As can been seen from the electrical spectra, a distinct clock component at 12.4 GHz is present. The low-frequency component in the spectra is also very high, which may fall in the passband of the EBPF, and thus, affect the clock recovery. To suppress these undesirable components, we can insert a section of polarization-maintaining fiber (PMF) between

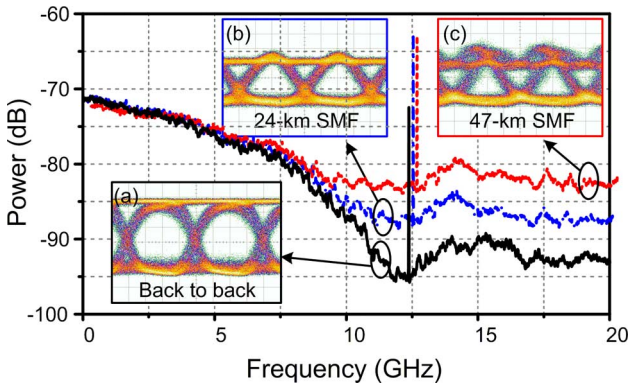

Fig. 2. Eye diagrams and electrical spectra of a typical optical NRZ signal (a) before transmission, (b) after 24-km SMF transmission, and (c) after 47-km SMF transmission.

PC2 and polarizer 2 (Pol2). The PMF and the polarizer would form an asymmetrical Mach–Zehnder interferometer (AMZI), which can convert the NRZ signal to PRZ signal, to enhance the clock component in the injection signal [28].

When the optical NRZ signal containing a clock component at f_m is injected into the frequency-doubling OEO constructed by low-frequency devices with a highest operating frequency up to $f_m/2$, an oscillation exactly at $f_m/2$ would be started in the OEO, although the input optical signal contains no distinct $f_m/2$ component. This is because the randomization of the injected NRZ data signal and the noise in the OEO would occasionally introduce a very small $f_m/2$ component. Once the $f_m/2$ component is present, it would be captured and amplified by the OEO. The amplified $f_m/2$ component is then fed back into the PolM-based IM and modulates the later injected NRZ data signal. With the modulation, the $f_m/2$ component in the electrical modulation signal and the f_m component in the injection signal are mixed to generate a new $f_m/2$ component, which greatly enhances the existing $f_m/2$ component. This positive feedback would finally lead to an oscillation at the frequency of $f_m/2$, and thus, an electrical clock at $f_m/2$ is obtained.

Once the OEO is oscillating at $f_m/2$, the PolM-based IM would be driven by a clock with an angular frequency of $\omega_m/2$ ($\omega_m = 2\pi f_m$). The optical intensity transfer function of the IM can be written as [25]

$$T_i = \alpha\left[1+\cos\left(\beta\sin\frac{\omega_m t}{2}+\phi_i\right)\right] \tag{1}$$

where α is the transmission factor, β is the phase modulation index, and ϕ_i ($i=1$ or 2) is a static phase term introduced by the PCs placed before the polarizers. By choosing $\phi_1 = -\pi/2$ via tuning PC2 in the OEO loop, the feedback signal containing the $f_m/2$ component for the optoelectronic oscillation is obtained. Then, PC3 in the other branch is adjusted to obtain a desired ϕ_2 for the optical output. For different ϕ_2, the transmission curve is different. Generally, there are three special cases: 1) $\phi_2 = -\pi/2$ or $\pi/2$, the transmission function is the same as the expression of an RZ pulse train with a repetition rate of $f_m/2$; 2) $\phi_2 = \pi$, the transmission function is the same as the expression of a CSRZ pulse train with a repetition rate of f_m [29]; and 3) $\phi_2 = 0$ and $\beta = \pi/2$, the transmission function is the same as the expression of an RZ pulse train with a repetition rate of f_m [29].

According to the aforementioned analysis, if a strong optical NRZ data signal with a bit rate of f_m and a weak CW optical probe is injected into the frequency-doubling OEO, the OEO will be injection locked at $f_m/2$. The electrical clock with a frequency of $f_m/2$ will be fed back into the PolM-based IM via the RF port and modulates the later injected NRZ data signal and the optical probe. When we choose $\phi_2 = -\pi/2$ or $\pi/2$ by tuning PC3, the transmission function is the same as the expression of an RZ pulse train with a repetition rate of $f_m/2$. As a result, the CW probe light will be carved into an optical pulse train with a repetition rate of $f_m/2$. The prescaled optical clock is thus obtained. Meanwhile, the NRZ signal is also carved to be an RZ signal by the electrical clock in the PolM-based IM, where the bit rate is divided by 2; therefore, optical serial-to-parallel conversion is realized. On the other hand, when $\phi_2 = 0$ or π, the transmission function is the same as the expression of an RZ or CSRZ pulse train with a repetition rate of f_m. The CW optical probe will be then carved into an optical clock with a repetition rate of f_m. Line-rate optical clock recovery is achieved. At the same time, the NRZ signal is also converted to an RZ or CSRZ signal. NRZ-to-RZ/CSRZ conversion is thus implemented. According to [29], to obtain the RZ signal, the phase-modulation index of the PolM should be $\pi/2$, which can be accomplished by using EAs with a high saturation power.

It is known that the use of synchronous modulation can reduce the timing jitter, which is used for 2R regeneration (reamplification and retiming) along with an erbium-doped fiber amplifier (EDFA) [30], [31]. In the frequency-doubling OEO, when the extracted clock is fed to the PolM-based IM, a temporal window is formed to synchronously modulate the degraded optical signal. The temporal window would suppress the wings of the degraded signal and confine the optical energy in the correct time slot; therefore, a reduction in timing jitter and an improvement in extinction ratio are realized by the in-line synchronous modulation. Because the input signal is an NRZ signal, the synchronous modulation can also reshape the NRZ signal to RZ pulses. By controlling the amplitude of the electrical clock, the temporal window can be very narrow [32], which can greatly reduce the noises in both "0" and "1" bits. If we further convert the regenerated signal back to the NRZ signal using an RZ-to-NRZ conversion module [8], [9], 3R regeneration (reamplification, reshaping, and retiming) of the NRZ signal is achievable.

The implementation of the aforementioned functions, however, requires a precise control of the polarization state of the input signal. In practice, the polarization state of the input signal will change all the time due to the environmental variations. To solve the problem, an adaptive polarization control module may be employed.

B. *MultiChannel Signal Injection*

In [25], we have assumed that only a single channel signal is injected into the frequency-doubling OEO. Since the clock component in a data signal is much larger than other components and the 3-dB passband $\Delta f_{3\,\mathrm{dB}}$ of the EBPF is very narrow

($\Delta f_{3\,\mathrm{dB}} \leq 50$ MHz), we can simply represent the injection signal as the sum of dc and sinusoidal components as

$$p(t) \approx p_0 \left[1 + m_0 \sin(\omega_0 t + \phi_0) + m_1 \sin(2\omega_0 t + \phi_1)\right] \quad (2)$$

where p_0 is the average optical power, m_i ($i = 0, 1$) is the modulation depth and ϕ_0 and ϕ_1 are the phases of the ω_0 and $2\omega_0$ components, respectively. If multiple channels containing a clock component with the same frequency, but different phases are simultaneously injected to the OEO, the power of the combined signal is simply an addition of the optical powers of the multichannel signals because they are at different wavelengths, and therefore, incoherent. The injection signal can thus be expressed as

$$p(t) \approx \sum_{n=1}^{N} p_n [1 + m_{0n} \sin(\omega_0 t + \phi_{0n}) + m_{1n} \sin(2\omega_0 t + \phi_{1n})] \quad (3)$$

where p_n is the average optical power at the *n*th channel, *N* is channel number, m_{0n} and m_{1n} are the modulation depths and ϕ_{0n} and ϕ_{1n} are the phases of the ω_0 and $2\omega_0$ components, respectively.

Using the trigonometric relationship $\sin(x+y) = \sin x \cos y + \cos x \sin y$, (3) can be expanded as follows:

$$\begin{aligned} p(t) \approx & \sum_{n=1}^{N} p_n + \left(\sum_{n=1}^{N} p_n m_{0n} \cos\,\phi_{0n}\right) \sin\,\omega_0 t \\ & + \left(\sum_{n=1}^{N} p_n m_{0n} \sin\,\phi_{0n}\right) \cos\,\omega_0 t \\ & + \left(\sum_{n=1}^{N} p_n m_{1n} \cos\,\phi_{1n}\right) \sin\,2\omega_0 t \\ & + \left(\sum_{n=1}^{N} p_n m_{1n} \sin\,\phi_{1n}\right) \cos\,2\omega_0 t. \end{aligned} \quad (4)$$

Considering $a \sin x + b \cos x = \sqrt{a^2 + b^2} \sin(x + \phi)$, where $\phi = \arctan(b/a)$, we obtain

$$p(t) \approx p_0' \left[1 + m_0' \sin(\omega_0 t + \phi_0') + m_1' \sin(2\omega_0 t + \phi_1')\right] \quad (5)$$

where

$$p_0' = \sum_{n=1}^{N} p_n \quad (6a)$$

$$m_0' = \frac{\sqrt{\left(\sum_{n=1}^{N} p_n m_{0n} \cos\phi_{0n}\right)^2 + \left(\sum_{n=1}^{N} p_n m_{0n} \sin\,\phi_{0n}\right)^2}}{p_0'} \quad (6b)$$

$$\phi_0' = \arctan \frac{\sum_{n=1}^{N} p_n m_{0n} \sin\,\phi_{0n}}{\sum_{n=1}^{N} p_n m_{0n} \cos\,\phi_{0n}} \quad (6c)$$

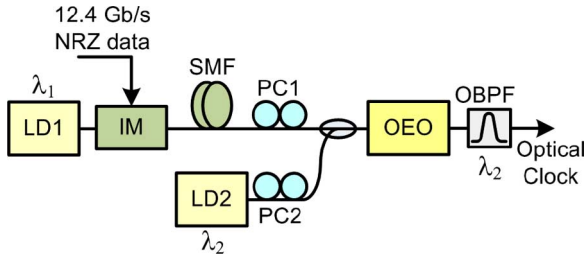

Fig. 3. Experimental setup to achieve the optical signal processing functions in an NRZ system based on a frequency-doubling OEO.

$$m_1' = \frac{\sqrt{\left(\sum_{n=1}^{N} p_n m_{1n} \cos\,\phi_{1n}\right)^2 + \left(\sum_{n=1}^{N} p_n m_{1n} \sin\,\phi_{1n}\right)^2}}{p_0'} \quad (6d)$$

and

$$\phi_1' = \arctan \frac{\sum_{n=1}^{N} p_n m_{1n} \sin\,\phi_{1n}}{\sum_{n=1}^{N} p_n m_{1n} \cos\,\phi_{1n}}. \quad (6e)$$

As can be seen, (5) has a similar expression as (2). Using the theory in [25], the frequency-doubling OEO can also be injection locked by the multichannel NRZ signals. Since there are no wavelength-dependent devices in the OEO, simultaneous multichannel optical signal processing, including clock recovery, NRZ-to-RZ/CSRZ format conversion, serial-to-parallel conversion, and optical signal regeneration, can be performed in a single OEO. It should be noted that NRZ-to-RZ/CSRZ format conversion, serial-to-parallel conversion, and optical signal regeneration would require that the input multichannel signals are temporally aligned, which can be realized by placing a synchronization module before the OEO.

III. Experimental Setup

Fig. 3 shows the experimental setup to achieve the proposed optical signal processing functions using the PolM-based frequency-doubling OEO. In the experiment, an optical NRZ data signal is obtained by modulating a CW light wave with an electrical NRZ data signal generated by a BER tester (BERT, Agilent N4901B) at a $LiNbO_3$ MZM. The wavelength of the CW light wave is 1555.7 nm. The data signal from the BERT is a pseudorandom bit sequence (PRBS) with a bit rate of 12.4 Gb/s and a word length of $2^{15} - 1$. The optical 12.4-Gb/s NRZ signal is then transmitted over a single-mode fiber (SMF) with a length of 23 or 47 km. The eye diagrams and the electrical spectra of the NRZ signal before and after transmission are shown in Fig. 2. To avoid the overlap of the spectra in Fig. 2, the electrical spectra of the NRZ signals are manually shifted by 0.1 GHz. As can be seen, all the signals have a distinct 12.4-GHz clock component. A CW optical probe from a tunable laser source along with the NRZ signal is sent to the PolM-based frequency-doubling OEO to perform clock recovery, format conversion, serial-to-parallel conversion, and synchronous modulation. The power of the optical NRZ signal is about 10 dBm and that of the CW light is about 0 dBm. The OEO has the same schematic

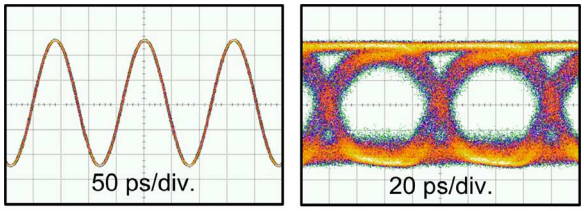

Fig. 4. (a) Waveform of the extracted electrical signal. (b) Eye diagram of the 12.4 Gb/s signal triggered by the OEO oscillating signal.

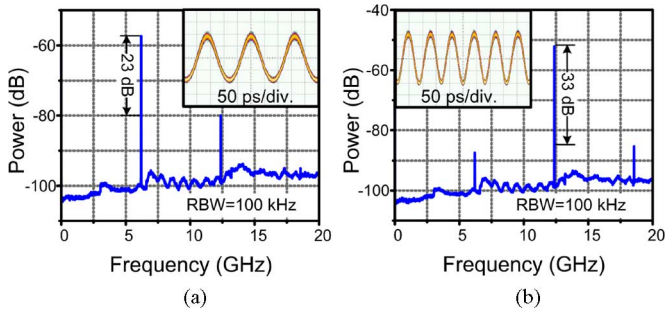

Fig. 5. Waveforms and electrical spectra of (a) the 6.2-GHz optical clock and (b) the 12.4-GHz optical clock.

diagram as that shown in Fig. 1, which consists of a PolM, three PCs, two polarizers, a PD, two EAs, an EBPF, a PS, and an electrical coupler. The parameters of the devices are as follows: the PD has a 3-dB bandwidth of 45 GHz and a responsibility of 0.4 A/W. The bandwidth of the EBPF is 20 MHz centered at ~6.2 GHz. The total small signal power gain of the EAs is about 85 dB. The free spectral range (FSR) of the OEO is measured to be 4.17 MHz. The PolM is a commercially available 40-Gbit/s GaAs-based PolM from Versawave Technologies [33]. The two polarizers are connected to the PolM via two PCs to form a dual-output-port IM. One output of the IM is connected to the RF port of the PolM to form an optoelectronic loop, and the other port serves as the output port for the processed signal. To select the desired wavelength, a tunable optical BPF with a 3-dB bandwidth of 0.3 nm is connected to the output port. An EDFA is used to increase the power of the optical signal to a satisfactory level.

To evaluate the performance of the output signal, a second 45-GHz PD (InGaAs/Schottky) is used to convert the optical signal to an electrical signal. The waveforms are observed by a high-speed sampling oscilloscope (Agilent 86116A), and the spectra are measured by an electrical spectrum analyzer (ESA; Agilent E4448A). In addition, an optical spectrum analyzer (Ando AQ 6317B) with a resolution of 0.01 nm is employed to monitor the optical spectra of the output signal.

IV. Results and Discussion

A. Prescaled and Line-Rate Clock Recovery

To extract the prescaled or line-rate clock from the input NRZ signal, the OEO must be first injection locked and produce an electrical prescaled clock signal at 6.2 GHz. To do so, we adjust PC2 in the OEO loop to make $\phi_1 = -\pi/2$. Fig. 4(a) shows the waveform of the OEO oscillating signal. The frequency is ~6.19 GHz, which is half the repetition rate of the injection signal considering the measurement error. To demonstrate that the OEO is operating in the injection-locked mode, the OEO oscillating signal is sent to the sampling oscilloscope as a trigger. Fig. 4(b) shows the 12.4-Gb/s data monitored with the sampling oscilloscope. The eye pattern is clear and widely open, and is almost the same as that in Fig. 2(a), indicating that the incoming data signal is well synchronized to the recovered clock. In the experiment, we introduce a time delay of 40 ps to the injection data signal. The obtained electrical clock also shifts about 40 ps, showing the clock is indeed extracted from the NRZ data signal. We also slightly vary the polarization states and the powers of the incident light wave and find no observable changes to the waveforms and spectra, thus demonstrating that the oscillation is very robust. The locking range of the OEO is measured to be (12.37186 and 12.37202 GHz), thus giving a locking bandwidth of 160 kHz. The locking bandwidth can be significantly extended if a section of PMF in the OEO loop is incorporated into the loop. To verify this conclusion, we insert a section of PMF with a differential group delay (DGD) of 20.1 ps into the OEO loop between the PolM and Pol2. By carefully adjusting the polarization states of the light wave before and after the PMF, the locking bandwidth is increased to ~300 kHz.

To generate the prescaled optical clock, we adjust PC3 in the output port to make $\phi_2 = -\pi/2$. Fig. 5(a) shows the temporal waveform and the electrical spectrum of the 6.2-GHz optical clock. Since the PC is tuned to generate the prescaled optical clock, the 6.2-GHz line is 23 dB higher than that of its second harmonic. To generate the line-rate optical clock at 12.4 GHz, PC3 is adjusted to make $\phi_2 = \pi$. The waveform and the electrical spectrum of the 12.4-GHz clock are shown in Fig. 5(b). Although the first- and third-order harmonics in the generated microwave signal are observed in the spectrum, they are 33 dB lower than that of the 12.4-GHz clock.

The stability of the clock recovery is investigated. The system is allowed to operate at a room environment for a period of 30 min, no significant variations in the waveform are observed. This is partly because the PolM-based IM requires no dc bias, which makes the system free from bias drifting. In addition, the total small signal gain of the EAs is very large; therefore, the EAs are highly saturated, thus making the oscillation very robust.

The phase noise performance of the recovered clock is also studied. Fig. 6 shows the single-sideband (SSB) phase noise spectra of the generated 6.2- and 12.4-GHz clocks, which are measured by a signal source analyzer (Agilent E5052B) incorporating a frequency downconverter (Agilent E5053A). The phase noises at an offset frequency of 10 kHz are –89 and −83.2 dBc/Hz for the prescaled clock at 6.2 GHz and the line-rate clock at 12.4 GHz, respectively. The 12.4-GHz clock has a 5.8-dB phase noise degradation. Theoretically, the phase noise of a frequency-doubled signal should have a phase noise degradation of $10\log_{10} 2^2 = 6$ dB. The measurement is

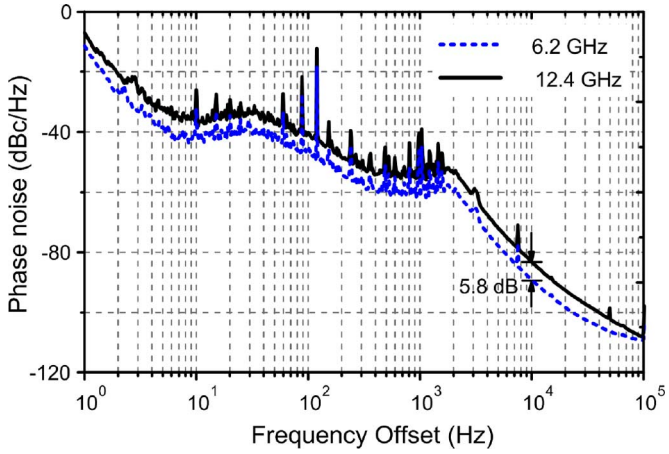

Fig. 6. SSB phase noise spectra of the recovered 6.2- and 12.4-GHz clocks.

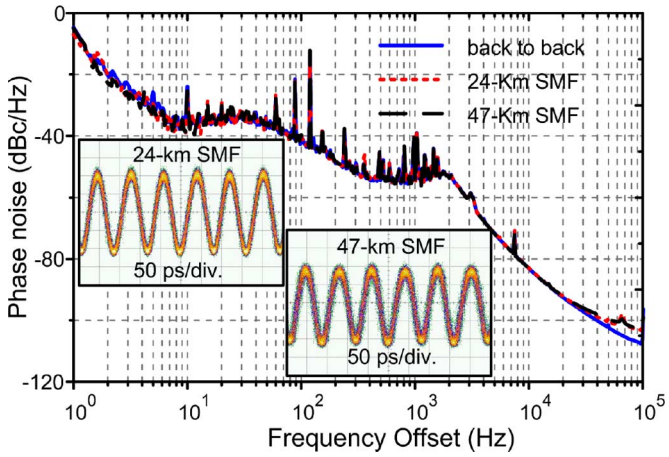

Fig. 7. SSB phase noise spectra of the 12.4-GHz clocks recovered from the back-to-back NRZ signal and the signal transmitted over 24- and 47-km SMF.

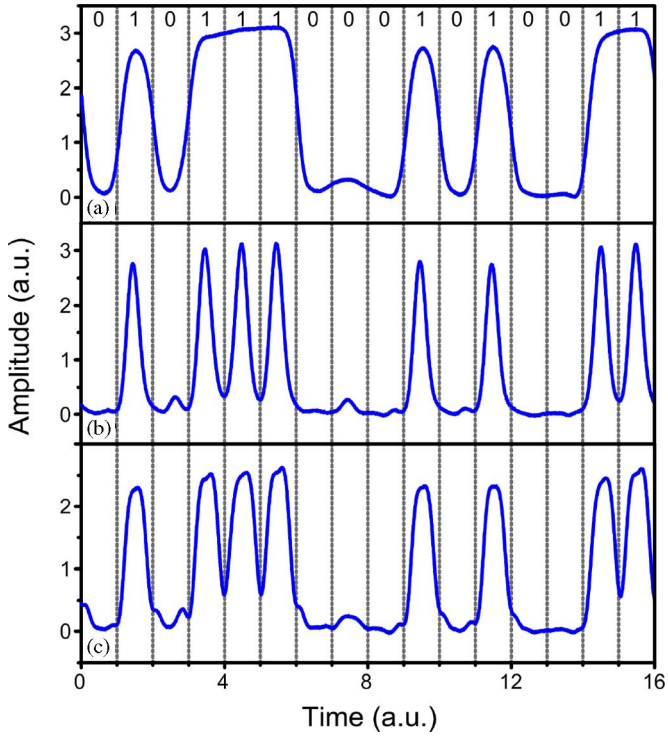

Fig. 8. Measured waveforms of (a) the original NRZ signal, (b) the converted RZ signal, and (c) the converted CSRZ signal.

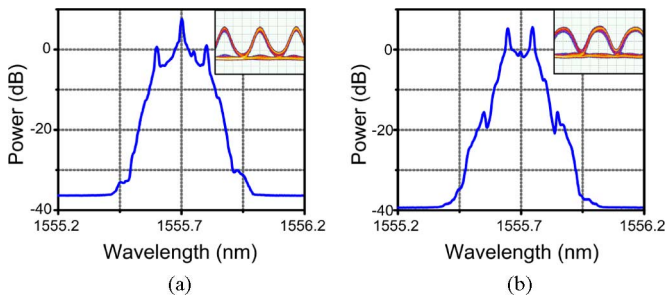

Fig. 9. Optical spectra and eye diagrams of (a) the converted RZ signal and (b) the converted CSRZ signal.

consistent with the theoretical prediction. Based on the spectral integration method [34] (from 10 Hz to 10 MHz), the *rms* timing jitters of the 6.2- and 12.4-GHz clocks are estimated to be 6.20 and 6.15 ps, respectively. It should be noted that the data signal generated by the BERT has a typical timing jitter of 9 ps; therefore, the OEO significantly reduces the timing jitter.

The injection locking status is maintained when a degraded signal is injected. Fig. 7 shows the SSB phase noise spectra of the generated 12.4-GHz clocks recovered from the back-to-back signal and the signals after 24- and 47-km transmission. As can be seen, the SSB phase noise spectra are almost the same for all the cases, thus indicating that the OEO has sufficient tolerance to the degradation of the input signal. This is because the OEO is a high-Q oscillator, which has a high sensitivity to be injection locked. The insets of Fig. 7 show the waveforms of the recovered clock from the degraded signals. Since the 24- and 47-km SMF used to degrade the injection signal introduces a slowly varied time shift within 16 ps, the temporal waveform is also shifted within 16 ps in the whole observation period, indicating again that the recovered clock is synchronized to the injection signal very well.

B. NRZ-to-RZ/CSRZ Conversion

To perform NRZ-to-RZ/CSRZ conversion, PC3 is carefully adjusted to make $\phi_2 = 0$ or π. The optical bandpass filter (OBPF) at the optical output port of the OEO is also tuned to select the data signal. Fig. 8 shows the waveforms of the original NRZ signal and the converted signal with a fixed pattern of "0101, 1100, 0101, 0011." As can be seen, the NRZ signal is successfully converted to RZ/CSRZ signal. The optical spectra and eye diagrams of the converted RZ and CSRZ signals are shown in Fig. 9. The full-widths at half-maximum (FWHMs) of the obtained RZ and CSRZ pulses are about 50 and 31 ps, respectively, corresponding to 62% and 38% of the bit period, respectively. The 1555.7-nm carrier in the CSRZ signal is suppressed by more than 13 dB, as compared with the carrier in the

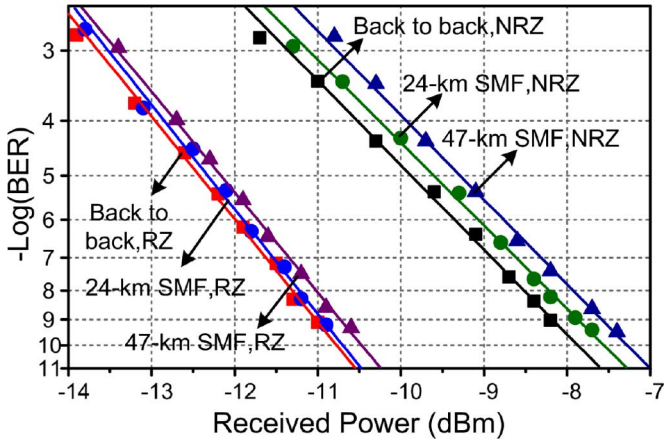

Fig. 10. BER curves of the NRZ signals before conversion and the RZ signals after conversion.

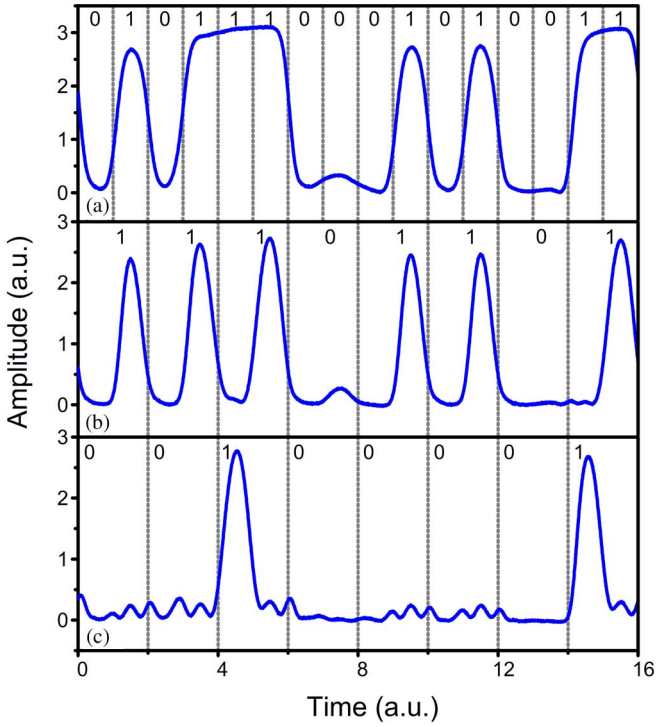

Fig. 11. Measured waveforms of (a) the original NRZ signal and (b) and (c) the serial-to-parallel converted signals.

RZ signal. It should be noted the CW probe light is not required for the NRZ-to-RZ/CSRZ conversion, since the conversion is directly performed on the input data signal, which saves a light source, as compared with the methods in [2]–[4]. Also, because the operation is directly performed on the input data signal, the NRZ-to-RZ/CSRZ conversion is optically transparent.

C. Synchronous Modulation

Since the NRZ-to-RZ conversion in our proposed OEO is also a synchronous modulation, the operation should be able to mitigate the optical impairments, which is confirmed by the BER measurement. To perform the BER measurement, the converted electrical signal after the 45-GHz PD is amplified by an EA with a 3-dB bandwidth of 10 GHz and a small signal gain of more than 25 dB. A clock data recovery module that is built in the BERT is also employed to retime the data signal before it is sent to a decision gate for BER measurement. Fig. 10 shows the BER curves of the NRZ signals before conversion and the RZ signals after conversion. As can be seen, the converted RZ signal from the back-to-back NRZ signal has a 2.89-dB improvement in receiver sensitivity. Ideally, the sensitivity improvement of the receiver between the NRZ and the 38% RZ format should be larger than 3 dB. However, the shot noise in the receiver, which is higher for a pulse with a larger amplitude, would reduce the receiver sensitivity improvement.

To demonstrate that the OEO-based signal processing module can perform signal regeneration, the back-to-back NRZ signal is degraded by transmission over a 24- or 47-km SMF. The transmission over a 24- or 47-km SMF introduces a power penalty of 0.35 or 0.59 dB at a 10^{-10} BER level. The penalty mainly originates from intersymbol interferences, timing jitter, and amplitude noise caused by fiber dispersion and the amplified spontaneous emission of EDFA. Since these impairments can be reduced by synchronous modulation, the improvement of the receiver sensitivity should be greater than the receiver sensitivity improvement for the back-to-back case, i.e., more than 2.89 dB. From Fig. 10, we can obtain that the receiving sensitivities are improved by 3.17 and 3.18 dB, thus confirming the signal quality improvement due to the regeneration. The sensitivity improvement can be further increased by using EAs with a larger saturation power in the OEO loop, which would form a narrower switching window [32].

D. Serial-to-parallel Conversion

To realize serial-to-parallel conversion, PC3 is adjusted to make $\phi_2 = -\pi/2$ or $\pi/2$. Fig. 11 shows the waveforms of the original serial NRZ signal and the converted parallel RZ signals. The original signal has a fixed pattern of "0101, 1100, 0101, 0011," while the pattern in the converted signals can be read as "1110, 1101" and "0010, 0001," confirming that the 1:2 serial-to-parallel conversion is achieved. The FWHMs of the pulses in the converted signals are 61.4 and 61.0 ps, corresponding to 38.1% and 37.8% of the bit period, respectively. It is important to note that the two parallel signals can be obtained simultaneously by replacing the polarizer with a polarization beam splitter with two output ports [26].

E. Multichannel Operation

Because there are no wavelength-dependent devices in the OEO loop, the OEO can extract the clock from a multichannel NRZ signal, and simultaneous multichannel signal processing is possible. For instance, Fig. 12 shows the optical spectra of the RZ/CSRZ signals converted from a dual-wavelength NRZ signal. The wavelength spacing is 0.75 nm. From Fig. 12, it can be seen that the optical carriers in the CSRZ signal are suppressed by more than 15 dB, as compared with the carriers in the RZ signal. By fixing the wavelength of one channel at

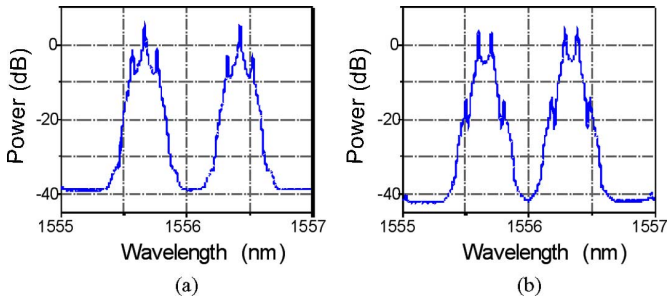

Fig. 12. Simultaneous dual-wavelength NRZ-to-RZ/CSRZ conversion. The optical spectrum of the converted (a) RZ signal and (b) CSRZ signal.

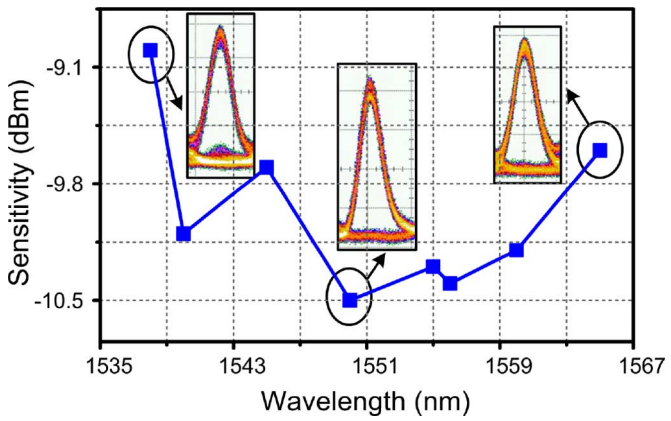

Fig. 13. Receiver sensitivity versus the wavelength of the injection NRZ signal.

1555.6 nm, we measure the receiver sensitivity of the converted signal in the other channel. The results are shown in Fig. 13. When the wavelength of the injection NRZ signal in that channel varied from 1538 to 1565 nm (wavelength spacing from 0.4 to 18 nm), the change of the receiver sensitivity is within 1.5 dB, thus showing that the scheme is suitable for multichannel signal processing in the C-band.

V. Conclusion

We have proposed and demonstrated a novel optical signal processing subsystem based on a frequency-doubling OEO for NRZ communication system applications. Several optical signal processing functions, including prescaled and line-rate clock recovery, NRZ-to-RZ/CSRZ conversion, 1:2 serial-to-parallel conversion, and synchronous modulation-based optical regeneration, were implemented using a frequency-doubling OEO with only low-frequency devices. Dual-wavelength operation with the wavelength spacing varying from 0.4 to 18 nm was studied. The change in the receiver sensitivity was less than 1.5 dB, showing that the scheme is suitable for multichannel signal processing. The proposed approach also features a simple and compact structure with stable and flexible operation, which may find applications in future optical communications systems.

References

[1] G. Bosco, A. Carena, V. Curri, R. Gaudino, and P. Poggiolini, "On the use of NRZ, RZ, and CSRZ modulation at 40 Gb/s with narrow DWDM channel spacing," *J. Lightw. Technol.*, vol. 20, no. 9, pp. 1694–1704, Sep. 2002.

[2] W. Li, M. H. Chen, Y. Dong, and S. Z. Xie, "All-optical format conversion from NRZ to CSRZ and between RZ and CSRZ using SOA-based fiber loop mirror," *IEEE Photon. Technol. Lett.*, vol. 16, no. 1, pp. 203–205, Jan. 2004.

[3] H. K. Lee, K. H. Kim, J. T. Ahn, M. Y. Jeon, and E. H. Lee, "All-optical format conversion from NRZ to RZ signals using a walk-off balanced nonlinear fibre loop mirror," *Electron. Lett.*, vol. 32, no. 25, pp. 2335–2336, Dec. 1996.

[4] T. Silveira, A. Ferreira, A. Teixeira, and P. Monteiro, "40-Gb/s multichannel NRZ to CSRZ format conversion using an SOA," *IEEE Photon. Technol. Lett.*, vol. 20, no. 19, pp. 1597–1599, Oct. 2008.

[5] T. Ye, C. S. Yan, Y. Y. Lu, F. F. Liu, and Y. K. Su, "All-optical regenerative NRZ-to-RZ format conversion using coupled ring-resonator optical waveguide," *Opt. Exp.*, vol. 16, no. 20, pp. 15325–15331, Sep. 2008.

[6] Y. Yu, X. L. Zhang, J. B. Rosas-Fernandez, D. X. Huang, R. V. Pemty, and I. H. White, "Simultaneous multiple DWDM channel NRZ-to-RZ regenerative format conversion at 10 and 20 Gb/s," *Opt. Exp.*, vol. 17, no. 5, pp. 3964–3969, Mar. 2009.

[7] B. Sartorius, "3R All-optical signal regeneration," in *Proc. ECOC*, 2001, pp. 98–125.

[8] M. Funabashi, Z. Q. Zhu, Z. Pan, L. Paraschis, and S. J. B. Yoo, "Optical clock recovery and 3R regeneration for 10-Gb/s NRZ signal to achieve 10 000-hop cascadability and 1 000 000-km transmission," *IEEE Photon. Technol. Lett.*, vol. 18, no. 20, pp. 2078–2080, Oct. 2006.

[9] H. S. Chung, R. Inohara, K. Nishimura, and M. Usami, "40-Gb/s NRZ wavelength conversion with 3R regeneration using an EA modulator and SOA polarization-discriminating delay interferometer," *IEEE Photon. Technol. Lett.*, vol. 18, no. 2, pp. 337–339, Jan. 2006.

[10] R. Takahashi and H. Suzuki, "1-Tb/s 16-b all-optical serial-to-parallel conversion using a surface-reflection optical switch," *IEEE Photon. Technol. Lett.*, vol. 15, no. 2, pp. 287–289, Feb. 2003.

[11] H. Hu, J. L. Yu, L. T. Zhang, A. X. Zhang, W. R. Wang, J. Wang, Y. Jiang, and E. Z. Yang, "40-Gb/s all-optical serial-to-parallel conversion based on a single SOA," *IEEE Photon. Technol. Lett.*, vol. 20, no. 13–16, pp. 1181–1183, Jul./Aug. 2008.

[12] L. Huo, Y. Dong, C. Y. Lou, and Y. Z. Gao, "Clock extraction using an optoelectronic oscillator from high-speed NRZ signal and NRZ-to-RZ format transformation," *IEEE Photon. Technol. Lett.*, vol. 15, no. 7, pp. 981–983, Jul. 2003.

[13] X. S. Yao and L. Maleki, "Optoelectronic oscillator for photonic systems," *IEEE J. Quantum Electron.*, vol. 32, no. 7, pp. 1141–1149, Jul. 1996.

[14] X. S. Yao and L. Maleki, "Multiloop optoelectronic oscillator," *IEEE J. Quantum Electron.*, vol. 36, no. 1, pp. 79–84, Jan. 2000.

[15] X. S. Yao and G. Lutes, "A high-speed photonic clock and carrier recovery device," *IEEE Photon. Technol. Lett.*, vol. 8, no. 5, pp. 688–690, May 1996.

[16] Z. X. Wang, T. Wang, C. Y. Lou, L. Huo, and Y. Z. Gao, "A novel approach for clock recovery without pattern effect from degraded signal," *Opt. Commun.*, vol. 219, no. 1–6, pp. 301–306, Apr. 2003.

[17] H. Tsuchida, "160-Gb/s optical clock recovery using a regeneratively mode-locked laser diode," *IEEE Photon. Technol. Lett.*, vol. 18, no. 16, pp. 1687–1689, Aug. 2006.

[18] J. Yu, K. Kojima, N. Chand, A. Ougazzaden, C. W. Lentz, J. M. Geary, J. M. Freund, and B. Mason, "Simultaneous demultiplexing and clock recovery of 80 Gb/s OTDM signals using a tandem electro-absorption modulator," in *Proc. 14th Annu. Meet. IEEE Lasers Electr.-Opt. Soc.*, San Diego, CA, 2001, pp. 358–359.

[19] C. Y. Lou, L. Huo, G. Q. Chang, and Y. Z. Gao, "Experimental study of clock division using the optoelectronic oscillator," *IEEE Photon. Technol. Lett.*, vol. 14, no. 8, pp. 1178–1180, Aug. 2002.

[20] S. L. Pan, L. Huo, Y. Yang, C. Lou, and Y. Gao, "First- and second-order PMD mitigation using 3R regeneration," *Proc. SPIE*, vol. 6021, pp. 602108-1–602108-6, 2005.

[21] T. Sakamoto, T. Kawanishi, and M. Izutsu, "Optoelectronic oscillator using push-pull Mach-Zehnder modulator biased at point for optical two-tone signal generation," in *Proc. Conf. Lasers Electr.-Opt. (CLEO 2005)*, vol. 2, pp. 877–879.

[22] H. Tsuchida, "Subharmonic optoelectronic oscillator," *IEEE Photon. Technol. Lett.*, vol. 20, no. 17, pp. 1509–1511, Sep. 2008.
[23] M. Shin, V. Grigoryan, and P. Kumar, "Frequency-doubling optoelectronic oscillator for generating high-frequency microwave signals with low phase noise," *Electron. Lett.*, vol. 43, no. 4, pp. 242–244, Feb. 2007.
[24] S. L. Pan and J. P. Yao, "A frequency-doubling optoelectronic oscillator using a polarization modulator," *IEEE Photon. Technol. Lett.*, vol. 21, no. 13, pp. 929–931, Jul. 2009.
[25] S. L. Pan and J. P. Yao, "Optical clock recovery using a polarization-modulator-based frequency-doubling optoelectronic oscillator," *J. Lightw. Technol.*, vol. 27, no. 16, pp. 3531–3539, Aug. 2009.
[26] H. Tsuchida, "Simultaneous prescaled clock recovery and serial-to-parallel conversion of data signals using a polarization modulator-based optoelectronic oscillator," *J. Lightw. Technol.*, vol. 27, no. 17, pp. 3777–3782, Aug. 2009.
[27] B. Franz, "Optical signal processing for very high speed (>40 Gbit/s) ETDM binary NRZ clock recovery," in *Proc. OFC 2001*, pp. MG1-1–MG1-3, Paper MG1-1.
[28] H. K. Lee, J. T. Ahn, M. Y. Jeon, K. H. Lim, D. S. Lim, and C. H. Lee, "All-optical clock recovery from NRZ data of 10 Gb/s," *IEEE Photon. Technol. Lett.*, vol. 11, no. 6, pp. 730–732, Jun. 1999.
[29] C. Y. Yu, Y. X. Wang, Z. Q. Pan, T. Luo, S. Kumar, B. Zhang, and A. E. Willner, "Carrier-suppressed 160 GHz pulse-train generation using a 40 GHz phase modulator with polarization-maintaining fiber," *Opt. Lett.*, vol. 34, no. 11, pp. 1657–1659, Jun. 2009.
[30] M. Nakazawa, K. Suzuki, and H. Kubota, "160Gbit/s (80 Gbit/s × 2 channels) WDM soliton transmission over 10000 km using in-line synchronous modulation," *Electron. Lett.*, vol. 35, no. 16, pp. 1358–1359, Aug. 1999.
[31] M. Matsumoto, "Polarization-mode dispersion mitigation by a fiber-based 2R regenerator combined with synchronous modulation," *IEEE Photon. Technol. Lett.*, vol. 16, no. 1, pp. 290–292, Jan. 2004.
[32] S. L. Pan and J. P. Yao, "Generation of chirp-free short optical pulse train with tunable pulse width based on a polarization modulator and an intensity modulator," *Opt. Lett.*, vol. 34, no. 14, pp. 2186–2188, Jul. 2009.
[33] J. D. Bull, N. A. Jaeger, H. Kato, M. Fairburn, A. Reid, and P. Ghanipour, "40-GHz electro-optic polarization modulator for fiber optic communications systems," in *Proc. SPIE*, vol. 5577, pp. 133–143, Dec. 2004.
[34] M. Jinno, "Correlated and uncorrelated timing jitter in gain-switched laser-diodes," *IEEE Photon. Technol. Lett.*, vol. 5, no. 10, pp. 1140–1143, Oct. 1993.

Shilong Pan (S'06–M'09) received the B.S. and Ph.D. degrees in electronics engineering from Tsinghua University, Beijing, China, in 2004 and 2008, respectively.

Since August 2008, he has been a Postdoctoral Research Fellow with the Microwave Photonics Research Laboratory, School of information Technology and Engineering, University of Ottawa, Ottawa, ON, Canada. His current research interests include ultra-wide band over fiber, ultrafast optical signal processing, fiber lasers, and terahertz wave generation.

Dr. Pan is a member of Optical Society of America and IEEE Laser and Electro-Optics Society.

Jianping Yao (M'99–SM'01) received the Ph.D. degree in electrical engineering from the Université de Toulon, Toulon, France, in 1997.

Since 2001, he has been with the School of Information Technology and Engineering, University of Ottawa, Ontario, Canada, where he is currently a Professor, Director of the Microwave Photonics Research Laboratory, and the Director of the Ottawa-Carleton Institute for Electrical and Computer Engineering, Ottawa. From 1999 to 2001, he was in the faculty with the School of Electrical and Electronic Engineering, Nanyang Technological University, Singapore. He is also a Yongqian Endowed Visiting Chair Professor with Zhejiang University, Hangzhou, China. In 2005, he was an invited Professor for three months with the Institut National Polytechnique de Grenoble, Grenoble, France. His current research interests include microwave photonics, which includes all-optical microwave signal processing, photonic generation of microwave, mm-wave and THz, radio over fiber, ultra-wide band over fiber, fiber Bragg gratings for microwave photonics applications, and optically controlled phased-array antenna, fiber lasers, fiber-optic sensors, and biophotonics. He has authored or coauthored more than 130 papers in refereed journals and more than 120 papers in conference proceeding.

Dr. Yao is a Registered Professional Engineer in the State of Ontario. He is a Fellow of Optical Society of America and a Senior Member of IEEE Photonics Society and IEEE Microwave Theory and Techniques Society. He is an Associate Editor of the International Journal of Microwave and Optical Technology. He is on the Editorial Board of IEEE TRANSACTIONS ON MICROWAVE THEORY AND TECHNIQUES. He was the recipient of the 2005 International Creative Research Award of the University of Ottawa, the 2007 George S. Glinski Award for Excellence in Research, and an Natural Sciences and Engineering Research Council of Canada Discovery Accelerator Supplements award in 2008. He was named University Research Chair in Microwave Photonics in 2007.